J. Wind Eng. Ind. Aerodyn. 98 (2010) 903–910

Contents lists available at ScienceDirect

Journal of Wind Engineering and Industrial Aerodynamics

journal homepage: www.elsevier.com/locate/jweia

Dispersion in a street canyon for a wind direction parallel to the street axis

L. Soulhac, P. Salizzoni *

Laboratoire de Mécanique des Fluides et d'Acoustique, Université de Lyon CNRS, École centrale de Lyon, INSA Lyon, Université Claude Bernard Lyon I 36, avenue Guy de Collongue, 69134 Ecully, France

ARTICLE INFO

Article history:
Received 26 January 2010
Received in revised form
10 September 2010
Accepted 14 September 2010
Available online 12 October 2010

Keywords:
Street canyon
Pollutant dispersion
Analytical model
Urban canopy flow

ABSTRACT

We investigate pollutant dispersion in a street canyon for an external wind direction parallel to the street axis, a case which has been poorly documented in the literature. The study is performed numerically and analytically by means of a model based on a series of simplifying assumptions. The range of validity of these assumptions is discussed by comparing analytical and numerical results for two different street aspect ratios. Our results show that, for a critical length of the street, ground level concentration can be higher than those observed in a street canyon whose axis is perpendicular to the external wind direction. We show that this critical length depends on the street aspect ratio.

1. Introduction

Most modelling studies on street canyons focus on the case of an external wind blowing perpendicularly to the axis of the street at roof-top level. This is generally assumed to be the worst case scenario for pollutant dispersion. In these conditions the mean convective transport along the street axis is almost zero and transfer of pollutant out of the street is mainly due to the turbulent exchanges at roof level. Therefore the pollutant particles are trapped in the recirculating motion within the street, resulting in high ground level concentrations. Pollutant dispersion in these flow conditions has been extensively studied experimentally and numerically and several analytical models have been developed in order to compute ground level pollutant concentrations (Vardoulakis et al., 2003).

Conversely, the case of a wind direction parallel, or 'nearly parallel', to the street axis is much less documented in the literature. 'Nearly parallel' denotes the cases in which the external wind is blowing in the range of incident angles producing a strong channeling of the pollutant plume within the street where the source is located. This range is of about $\pm 2.5^\circ$ for extremely regular obstacle arrays (Garbero et al., 2010). However, in field studies, the minimal accuracy adopted in defining different classes of wind directions is $\pm 10^\circ$ (Berkowicz et al., 1996, 2002). It is worth noting that in a typical European city such as Lyon, the condition of a wind 'nearly' parallel to the street axis occurs quite often and, as it is shown in Fig. 1, this is as frequent as that of a perpendicular wind.

For the case of parallel wind as far as we are aware, the only analytical models are those proposed by Hargreaves and Baker (1997) and Berkowicz et al. (1997). However, early field experimental results suggest that the case of a wind direction parallel to the street axis may result in even more critical conditions for pollutant dispersion. Experiments performed in a Nantes street showed that the concentrations were highest for an external wind direction parallel to the street axis (Baranger, 1986). Similarly, in situ observations in Copenhagen (Berkowicz et al., 1994, 1996) showed that, for a given number of streets, the measured maximal concentration occurred when the wind was parallel rather than perpendicular to the street axis. For this reason the street-canyon model OSPM, validated on the basis of these in situ experiments in regular street canyons (aspect ratio $\sim$ unity), predicts maximum concentration levels when the wind is parallel to the street (Berkowicz et al., 1997). More recently, more extensive in situ experimental campaigns were performed providing additional information on the dependence of ground level on wind speed and directions (Berkowicz et al., 2002; Kumar et al., 2008; Tomlin et al., 2009; Martin et al., 2009).

These results show that an external wind parallel to the street axis does not necessarily result in enhanced street ventilation compared to the case of a perpendicular wind. To explain this we consider the idealised case of a street with a steady and semi-infinite line source of pollutant within it. Pollutants are transported along the street by the mean flow and cause the concentration to increase with distance from the upwind limit of the pollutant source. If the street is sufficiently long, after a given distance, the pollutant concentration can exceed that

* Corresponding author.
E-mail address: pietro.salizzoni@ec-lyon.fr (P. Salizzoni).

0167-6105/$ - see front matter © 2010 Elsevier Ltd. All rights reserved.
doi:10.1016/j.jweia.2010.09.004

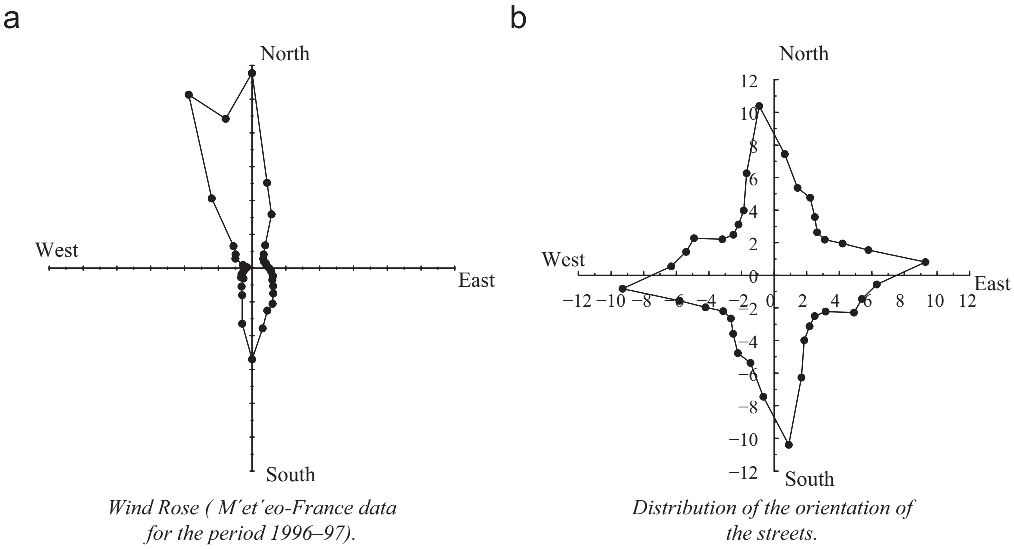

Fig. 1. Street orientation and wind rose in Lyon. (a) Wind Rose (Météo-France data for the period 1996–1997). (b) Distribution of the orientation of the streets.

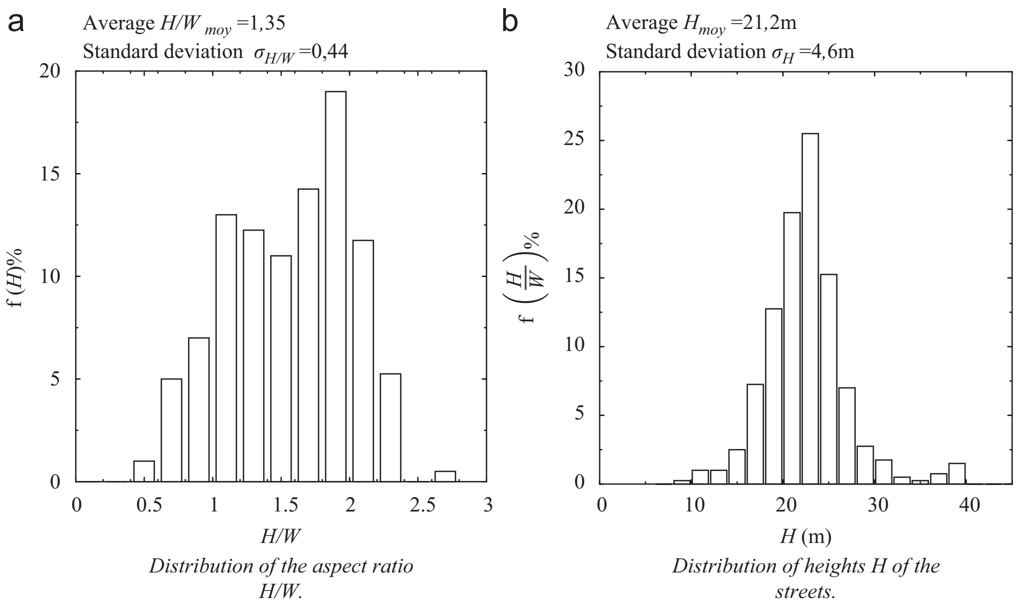

Fig. 2. Geometrical characteristics of the streets in a central district in Lyon (6th Arrondissement). (a) Distribution of the aspect ratio H/W. (b) Distribution of heights H of the streets.

observed for an external wind blowing perpendicularly with respect to the street axis.

To investigate pollutant dispersion in a street canyon with a parallel wind we have developed an analytical model and performed numerical simulations. The model is based on simplifying assumptions (Section 2) whose validity is analysed by comparing analytical and numerical results (Section 3). In order to critically discuss the numerical and the analytical results (Section 4) we refer to a data set characterising the geometry of the streets of a real city. These data (Soulhac, 2000) concern the city of Lyon (France) whose characteristics are representative of a large number of European cities. The data set provide information on the street aspect ratio of the streets (Fig. 2a) and on the height of the buildings (Fig. 2b) in a central district of Lyon and on the length of the streets over the whole urban area (Fig. 3). Conclusion are drawn in Section 5.

2. Analytical modelling

We aim to describe the non-uniform concentration field due to a steady release of pollutant with an analytical solution of the advection–diffusion equation. To that purpose we adopt a simplified description of the flow within the street and of the geometry of the street. We consider here an infinitely long two-dimensional symmetrical street, characterized by its height H and width W (see Fig. 4). We assume that the street is immersed in an urban canopy and overlain by a neutral atmospheric boundary layer. The coordinate system is defined in Fig. 4; the origin is located at the street level, at one side of the street, and the x-axis is oriented parallel to the street. In the following analysis we will focus on regular ($H/W=1$) and narrow canyon ($H/W=2$), on a range of aspect ratio typical for the central part of European cities (Fig. 2).

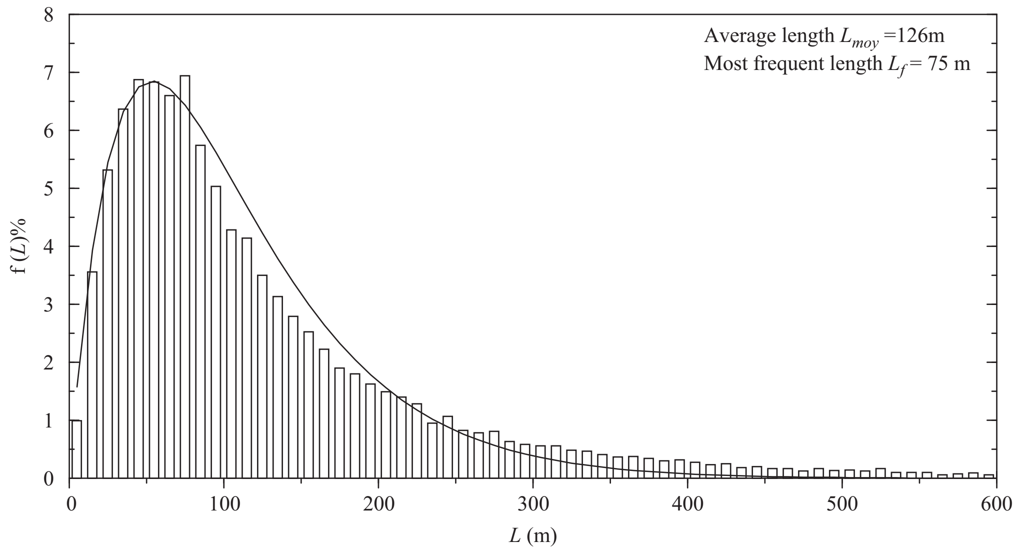

Fig. 3. Distribution of streets length in the urban area of Lyon; the solid lines correspond to the Gamma distribution with a mean value of 107 m.

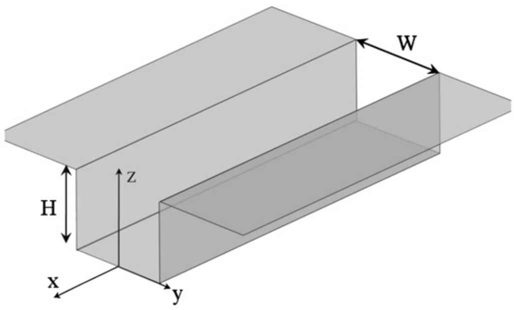

Fig. 4. Street geometry and co-ordinate system.

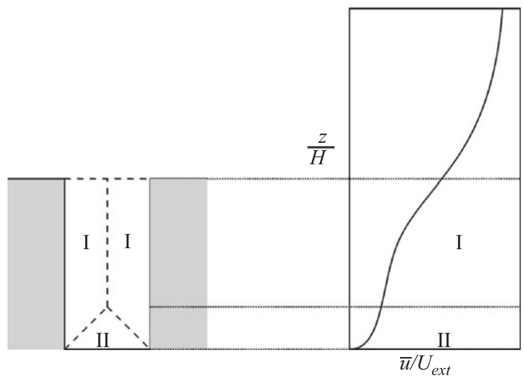

Fig. 5. Flow in a street parallel to the wind direction: influence regions and sketch of the vertical profile of mean velocity profile at the centre of the street.

The mean velocity components in the directions x, y and z are denoted by $\overline{u}$, $\overline{v}$ and $\overline{w}$, respectively (Fig. 4). The aerodynamic roughness of the side walls and floor of the canyon will be characterized by a roughness height z_i.

2.1. Velocity field

To model the flow within the street we apply the analytical solution developed by Soulhac et al. (2008). This model provides the distribution of the mean velocity $\overline{u}$ and of the turbulent diffusivity of momentum K as a function of the mean velocity at roof level, the canyon aspect ratio H/W and the roughness of the walls of the canyon. The main assumption of the model is that mean velocity field within the street (for $z<H$) is induced by a momentum transfer from the external wind; the incoming momentum is due only to turbulent entrainment, and this can be expressed by the shear stress τ_H, exerted by the external flow at roof level. Within the street, the no-slip condition is imposed on the internal faces of the canyon and generating boundary layers along the walls and the floor. In order to simplify the problem, it is assumed that each surface influences the flow only in part of the canyon. This is shown schematically in Fig. 5. The region of the flow influenced by the side walls is denoted Region I and the region influenced by the ground, Region II (it is worth noting that the relative importance of Regions I and II depends on the street geometry).

A brief description of the model is given in Appendix A. The solution for the velocity field (given by Eqs. (8-11) in Appendix A) is illustrated in Fig. 6, where velocity contours have been plotted for two different street aspect ratios ($H/W=2$ in Fig. 6a, $H/W=1$ in Fig. 6b). A full description and a detailed validation of the model by means of comparison with numerical simulations is provided by Soulhac et al. (2008).

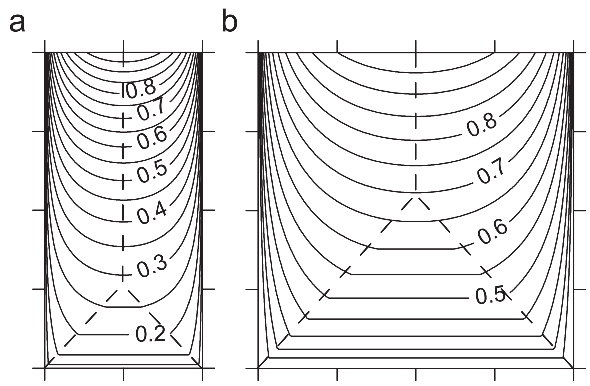

Fig. 6. Contours of dimensionless longitudinal velocity (normalised with U_m, the mean velocity at roof level and on the street axis) for the two different street aspect ratio: (a) $H/W=2$, (b) $H/W=1$.

According to the model, both $\overline{u}$ and K_s vary horizontally and vertically within the street (Fig. 6). However, analytical solutions of the advection–diffusion equation in a non-uniform flow are generally difficult to achieve. We therefore need to further simplify the description of the flow. To that purpose we compute a spatially averaged value of the flow variables defined as follows:

$$U = \int_{z=0}^{z=W} \int_{y=-W/2}^{Y=W/2} \overline{u}(y,z)\,dy\,dz \quad (1)$$

$$K = \int_{z=0}^{z=W} \int_{y=-W/2}^{Y=W/2} K_s(y,z)\,dy\,dz \quad (2)$$

In a regular square canyon ($H/W=1$) U and K represent an average over the whole section of the street. For a narrow canyon ($H/W=2$) U and K are representative of the lower half of the street (i.e. for $z \le H/2$), where most pollution receptors are located and which is therefore the region we are most interested in analysing.

2.2. Dispersion

We consider a line source of length L_s, aligned in the direction x of the flow, whose upstream end is located at the origin of the reference frame. The source uniformly emits a mass flow rate of contaminant per unit length Q. Firstly we obtain a solution for the case of open field without any solid boundaries. We then use this solution for the case of an infinite street length. In what follows we will assume that the turbulent Schmidt number is approximately 1 (Launder, 1978), i.e. that the turbulent diffusivity K_s of a scalar quantity can be considered equal to K, the turbulent diffusivity of momentum.

2.2.1. Line source in open field

Since we assume uniform mean velocity U and diffusivity K, the spatial distribution of pollutant concentration from a point source can be easily modelled by means of a Gaussian plume (Arya, 1999). For a linear, steady pollutant source, the concentration at the point of co-ordinates (x,y,z) is obtained by integrating the solution for a point source neglecting the contribution of diffusion in the stream-wise direction, i.e. $y^2+z^2 \ll (x-x_s)^2$:

$$\overline{c} = \int_0^{L_s} \frac{Q}{4\pi K(x-x_s)} \exp\left\{-\frac{U}{4K(x-x_s)}(y^2+z^2)\right\} dx_s \quad (3)$$

which gives

$$\begin{cases} \overline{c} = 0 & \text{if } x<0 \\ \overline{c} = \dfrac{Q}{4\pi K} E_1\left\{\dfrac{U}{4Kx}(y^2+z^2)\right\} & \text{if } 0 \le x < L_s \\ \overline{c} = \dfrac{Q}{4\pi K}\left[E_1\left\{\dfrac{U}{4Kx}(y^2+z^2)\right\} - E_1\left\{\dfrac{U}{4K(x-L_s)}(y^2+z^2)\right\}\right] & \text{if } L_s \le x \end{cases} \quad (4)$$

where E_1 is the first order *exponential integral* function. Alternatively, the distribution of the concentration can be computed by approximating the exponential integral function E_1 with a limited development close to the origin (Abramowitz and Stegun, 1965):

$$E_1(x) \simeq \ln\left(\frac{1}{x}\right) - \gamma + O(x^2) \quad \text{if } x \ll 1 \quad (5)$$

where $\gamma \simeq 0.577$ is the Euler constant and O is the Landau notation. The integral (3) can then be approximated by

$$\overline{c} \simeq \frac{Q}{4\pi K}\left[\ln\left(\frac{4Kx}{U(y^2+z^2)}\right) - \gamma\right] \quad \text{if } 0 \le x < L_s \quad \text{and} \quad y^2+z^2 \ll \frac{4Kx}{U} \quad (6)$$

2.2.2. Influence of the street walls

To take into account the effect of the ground and of the lateral street walls that impose a zero mass flux boundary condition, we use the method of images. This approach has been already applied by Hargreaves and Baker (1997) in their puff dispersion model. Since we are mainly interested in the concentrations close to the ground, we simplify the problem by assuming semi-infinite vertical walls (in the upwards direction). The image source is located symmetrically to the real source at the other side of the wall. When more than one wall is present, the problem becomes more complicated since it is necessary to include image sources of the images to satisfy the zero mass flux condition. For a source placed within the street, it is therefore necessary to take into account the reflection of the ground and a series of infinite reflections due to the vertical walls.

We refer to as C_{y_i,z_i} the contribution of an image source placed in (y_i,z_i) and given by Eq. (4). The pollutant concentration within the street C_{rue} due to a steady release from a line source placed at (y_s,z_s), can then be calculated as

$$C_{rue} = \sum_{i=-\infty}^{+\infty} (C_{[y_s+2iW],z_s} + C_{[y_s+2iW],-z_s}) + \sum_{i=-\infty}^{+\infty} (C_{[-y_s+(2i+1)W],z_s} + C_{[-y_s+(2i+1)W],-z_s}) \quad (7)$$

Since the contribution of higher order terms is negligible, we retain only the first 10 terms of this series.

3. Numerical simulations

In order to test the model, we have compared it with the results of numerical simulations performed using the code MERCURE (Carissimo et al., 1995; Milliez and Carissimo, 2007), a three-dimensional numerical code which implements a finite difference method to solve the Reynolds averaged Navier–Stokes equations with a standard $k-\varepsilon$ turbulence model. The pollutant source was placed at the centre of the street ($y=0$) and at ground level ($z=0$). Computations were performed for a source strength of $Q=0.002\,\text{kg}\,\text{s}^{-1}\,\text{m}^{-1}$, a street height $H=20$ m and for two street widths W ($W=10$ and 20 m). A non-regular mesh has been used and the size of the grid cell close to the rigid boundaries was set equal to $H/100$ whereas in the centre of the canyon its size was $H/20$. Two street geometry configurations have been tested, corresponding to different street aspect ratio $H/W=1$ and 2. The grid for the two cases is shown in Fig. 11.

The roughness lengths z_i of the roof and of the side wall of the street have been set equal to $2.5\times10^{-3}H$ (i.e. 5 cm). In order to define a solution independent of the initial conditions and of the longitudinal coordinate x, the flow was defined to be periodic in the x-direction.

4. Comparative discussion

In Figs. 8 and 9 are plotted cross-sections on the plane y–z of the non-dimensional mean concentration fields ($C^* = \overline{c}U_H W/Q$) within the canyon (i.e. $z/H<1$), for two different street aspect ratios ($H/W=1$ and 2), and for increasing distances from the origin $x=0$ of the semi-infinite line source. Qualitatively, Figs. 8 and 9 show that, for both configurations presented here, there is generally good agreement between the theoretical model and the numerical results. Significant difference between numerical and analytical results can be detected in the upper part of the canyon, as the plume reaches the roof level.

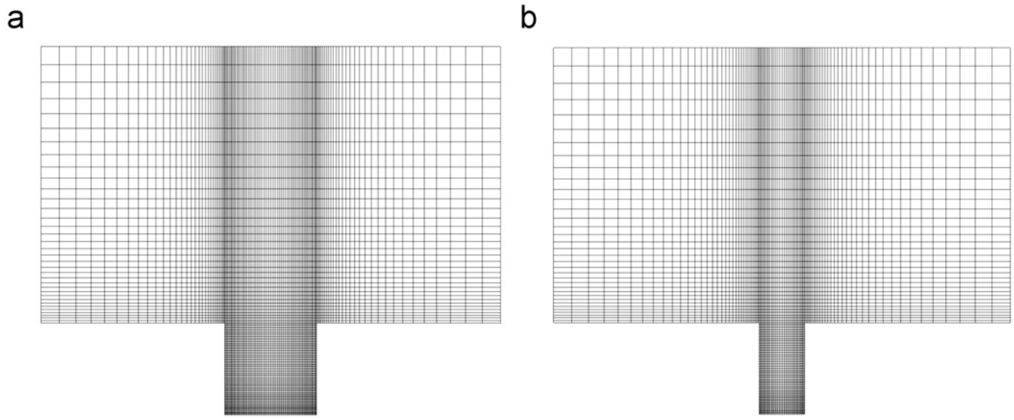

Fig. 7. Spatial discretisation for the numerical simulations for the (a) regular and the (b) narrow canyon.

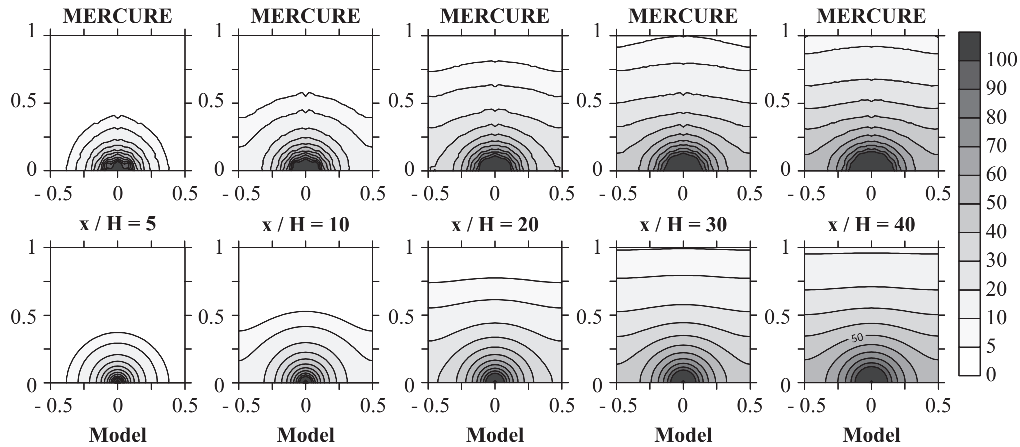

Fig. 8. Vertical cross-section of the non-dimensional mean concentration $C^* = \bar{c}U_H W/Q$ fields within a narrow canyon ($H/W = 1$), as a function of y/W and z/H. Comparison between numerical and analytical results.

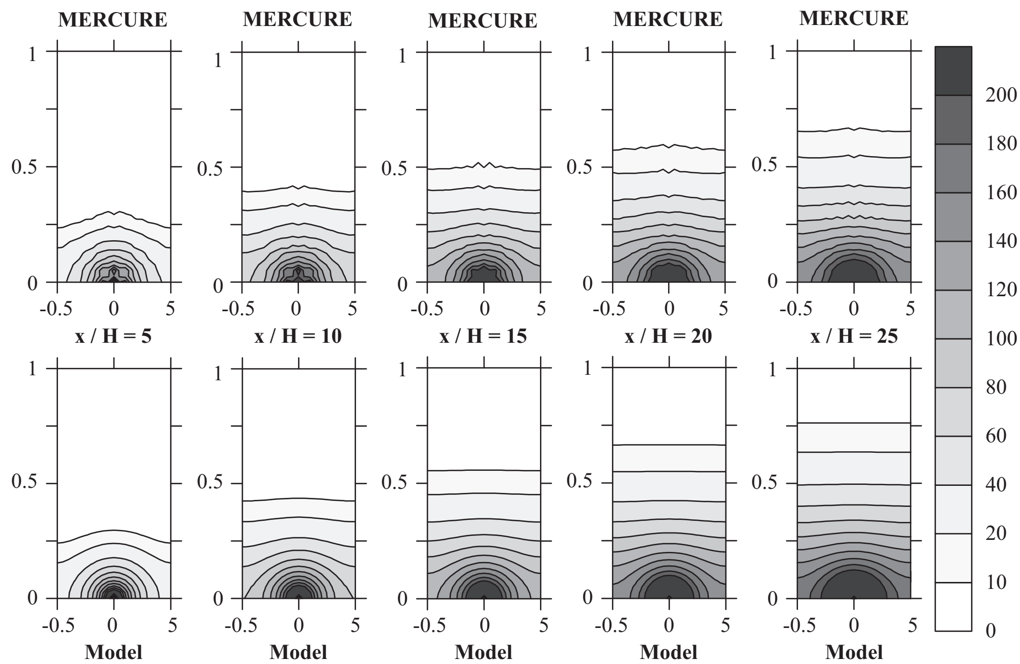

Fig. 9. Vertical cross-section of the non-dimensional mean concentration $C^* = \bar{c}U_H W/Q$ fields within a narrow canyon ($H/W = 2$), as a function of y/W and z/H. Comparison between numerical and analytical results.

In order to give a quantitative comparison between numerical and analytical results we show in Figs. 10 and 11 longitudinal profiles of the mean concentration for increasing distances from the origin $x=0$. The profiles are taken close to the street walls and for values of z/H and y/H representative of the human breathing zone.

When $H/W=1$ (Fig. 10a and b) the analytical solution agrees well with the numerical simulation up to a distance $x=35H$. This corresponds approximately to distance at which the standard deviation of the plume $\sqrt{2Kx/U}$ attains the street height H. Beyond this distance, the plume occupies the whole street and begins to spread out of it. The values of U and K adopted by the model are no longer representative of the dispersion process. At that distance the plume size encompasses the roof top and is therefore advected with a velocity that is significantly higher than the spatially averaged velocity within the canyon. Similarly the turbulent diffusivity adopted by the model is significantly smaller compared to that above the roof level. Finally we recall that our analytical assumes semi-infinite later canyon walls, which therefore inhibits the lateral spreading of the plume even for $z/H>1$. All these arguments provide reliable explanations for the overestimate of the concentrations by the model from a distance $x>35H$ from the source. Considering realistic values of H, K and U, this happens for distances x of few hundred meters, which therefore exceed the average length of a section of street in a European town (3).

These arguments are valid also for the narrow canyon, i.e. $H/W=2$ (Fig. 11a and b). However, in that case the street is twice as narrow as in the previous case, so that the distance required for the plume to occupy the whole street decreases fourfold. For this reason the model gives reliable results only up to a distance of approximately $10H$. This more rapid divergence between numerical and analytical results is also due to the fact that, for the narrow canyon, the spatially averaged values of $\overline{u}$ and K adopted in the analytical model are calculated only over the lower half of the street (Section 2.1).

Figs. 10 and 11 also show the range of values of concentration at ground level observed in the case of perpendicular wind. These values encompass typical concentrations registered in previous wind tunnel and numerical studies for both street aspect ratios (Pavageau and Schatzmann, 1999; Salizzoni, 2006; Soulhac et al., 2009; Salizzoni et al., 2009). Since the concentration increases indefinitely in the stream-wise direction x, the ground level concentrations become comparable to those observed in the case

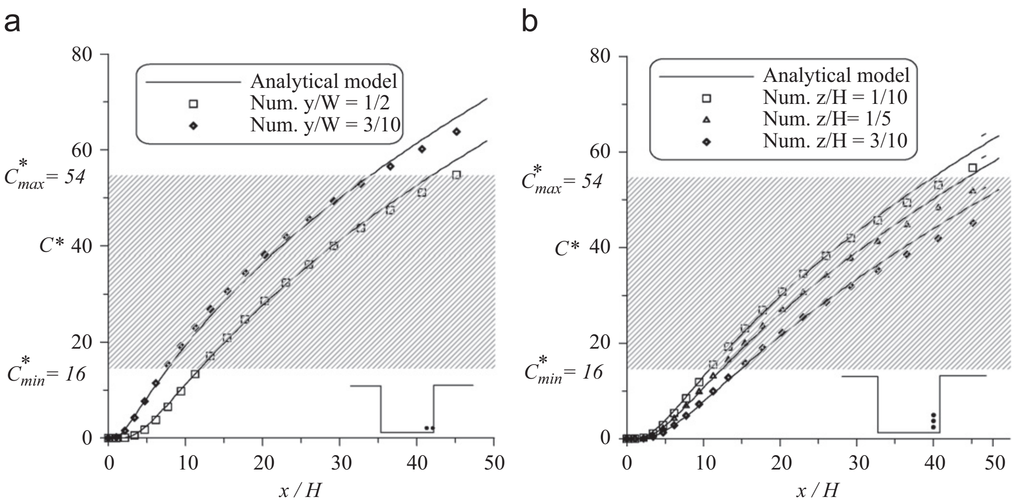

Fig. 10. Non-dimensional concentration $C^*=\overline{c}U_HW/Q$ along a street parallel to the external wind—comparison between analytical model and numerical simulations for a regular canyon; longitudinal mean concentration profiles at (a) $z/H=1/10$ and at (b) $y/W=2/5$.

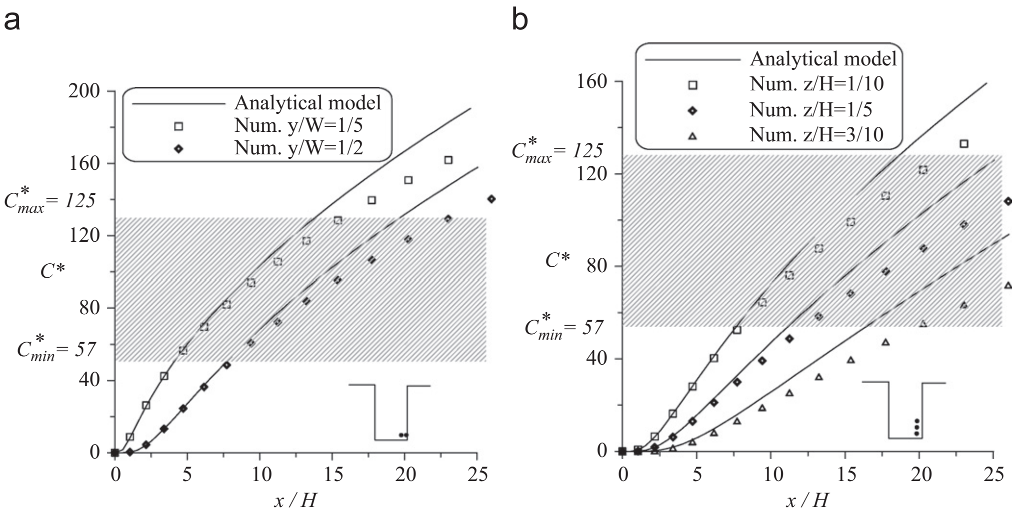

Fig. 11. Non-dimensional concentration $C^*=\overline{c}U_HW/Q$ along a street parallel to the external wind—comparison between analytical model and numerical simulations for the narrow canyon; longitudinal mean concentration profiles at (a) $z/H=1/10$ and at (b) $y/W=2/5$.

of a perpendicular external wind (Figs. 10 and 11). This occurs for $x/H \simeq 7$ for the narrow street and $x/H \simeq 12$ for a square street. Considering values of H between 15 and 20 m, which are representative of building heights in the centre of a typical European city as Lyon (Fig. 7b), this happens for streets approximately 100 m long for a narrow street, and 200 m for a regular street canyon. Furthermore, for long streets the ground level concentrations for a parallel wind may even exceed those registered for a perpendicular wind. In a narrow street ($H/W=2$) this would occur for a critical distance of approximately 250–300 m. As Fig. 3 shows, these are realistic values characterising the geometry of a significant part of the streets in urban areas. We therefore believe that this process of accumulation of pollutant can give rise to peak of ground level concentrations in real urban street canyons and explain the peaks observed in in situ experiments, as discussed in the Introduction of this study.

5. Conclusion

We studied pollutant dispersion within a street canyon whose axis is parallel to the external wind direction. We have developed a simple analytical model which allows us to compute the three-dimensional distribution of pollutant concentrations within an infinitely long street containing a semi-infinite ground level line source. The results of the model, which is based on a simplified description of the flow and of the canyon geometry, are compared with numerical simulations. Both analytical model and numerical simulations show that, from a given length of the canyon (that depends on the aspect ratio), the street ground level concentrations are close to those observed with a wind direction perpendicular to the street axis and may even exceed them. This analysis shows the importance of pollutant accumulation in a street canyon due to the mean advection along its axis which can attain (and even exceed) that caused by the recirculating motion induced by the wind component transverse to the street axis. The importance of the mean convective fluxes is not only confined to the case of infinite (or 'long') streets. In a real street of finite length, the role of advection along the street axis is crucial in defining pollutant fluxes at the downstream end, i.e. at the intersections, where the pollutants from the surrounding streets are mixed and transferred to the downstream streets. For these reasons a correct estimation of the pollutant fluxes along the street axis is essential in determining the pollutant transfer within the urban canopy and have therefore to be taken into account in urban dispersion models.

Appendix A

We briefly summarise here the analytical model of mean wind velocities and turbulent diffusivity developed by Soulhac et al. (2008), in case of an external wind parallel to the axis of the street. The model is based on two main assumptions:

- the flow in the street is driven by the turbulent entrainment at roof level under the forcing action of the overlying atmospheric boundary layer flow;
- the flow filed within the street can be divided into different regions, referred to as Regions I and II (Fig. 5), whose dynamics is considered as independent from the others and influenced only by the nearest rigid boundary.

The boundaries between the regions are defined geometrically, such that any point on a boundary between two regions is equidistant from the two surfaces that generate the two regions. For the case considered here ($H/W>1$), the vertical walls contribute more than the half of the total street perimeter and most of the flow within the street is therefore controlled by the side walls (Region I). The influence of the ground is confined to the lower part of the flow field (Region II). The mean velocity profile in the street centre can be considered as composed of two different regions (Fig. 5). It will be shown that, in Region I, the mean velocity profile can be modelled by means of an exponential law whilst in Region II, a log-law needs to be adopted.

We first consider the Region I, within which the velocity field is mainly influenced by the side walls. We assume that the mean horizontal velocity $\overline{u}$ and the turbulent diffusivity K can be expressed as follows:

$$\begin{cases} \overline{u} = U_m f(y^+) g(z^+) \\ K = K_m y^+ g(z^+) \end{cases} \tag{8}$$

where U_m and K_m are the velocity and diffusivity on the street centreline and at the interface with the external flow, and where $y^+ = y - W/2/\delta_i$ and $z^+ = z/\delta_i$ are the non-dimensional distances from the lateral wall and from the ground, respectively. These have been normalised with $\delta_i = \min(H, W/2)$, which represents the thickness of the boundary layer developing on the side walls. The form functions $f(y^+)$ and $g(z^+)$ in Eq. (8) are

$$\begin{cases} f(y^+) = \dfrac{J_1(C)Y_0(Cy^+) - J_0(Cy^+)Y_1(C)}{J_1(C)Y_0(C) - J_0(C)Y_1(C)} \\ g(z^+) = \exp\left[\dfrac{C}{\sqrt{2}}\left(z^+ - \dfrac{H}{\delta_i}\right)\right] \end{cases} \tag{9}$$

where J_0 and Y_0 are Bessel functions and C is a constant, which is related to the roughness of the walls and can be determined by solving the following non-linear equation (Soulhac et al., 2008):

$$\frac{z_i}{\delta_i} = \frac{2}{C}\exp\left[\frac{\pi}{2}\frac{Y_1(C)}{J_1(C)} - \gamma\right] \tag{10}$$

Concerning the Region II, we assume that the effect of the side walls does not have any influence on the lower part of the velocity field, close to ground level. The flow developing above the ground can then be modelled simply as a boundary layer over a rough wall. The vertical profiles of mean velocity and diffusiveness can therefore be modelled as

$$\begin{cases} \overline{u} = \dfrac{u_*^s}{\kappa}\ln\left(\dfrac{z}{z_i}\right) \\ K = \kappa u_*^s z \end{cases} \tag{11}$$

where u_*^s is the friction velocity and z_i is the roughness of the ground (which we assume identical to that of the lateral walls). The friction velocity u_*^s is determined by means of a matching with the profile in the Region I at the interface between the two regions, i.e. for $z = \delta_i$. We then obtain

$$u_*^s = U_m \frac{\kappa}{\ln\left(\dfrac{\delta_i}{z_i}\right)} \exp\left[\frac{C}{\sqrt{2}}\left(1 - \frac{H}{\delta_i}\right)\right] \tag{12}$$

The values of U_m and K_m can be obtained by matching the velocity profiles at the top of the canyon with that in the overlying atmospheric boundary layer flow. In order to match the velocity profile at the top of the canopy with the mean profile in the inertial region we assume that the Reynolds stress above the roof level is constant with height and equal to that in the inertial region $\tau_0 = \rho u_*^2$, being ρ the air density and u_* the friction velocity of the overlying atmospheric boundary layer. The latter is obtained by fitting the mean velocity vertical profile to the classical logarithmic law:

$$\overline{u} = \frac{u_*}{\kappa}\ln\left(\frac{z-d}{z_0}\right) \tag{13}$$

where κ is the von Kármán constant and d and z_0 are, respectively, the displacement height and the aerodynamic roughness of the surface of the urban canopy within which the street is immersed. The forcing condition imposes that the magnitude of these stress has to be equal to the stress $\tau_H(=\tau_0=\rho u_*^2)$ exerted by the overlying flow. Assuming a zero-order closure model, by means of Eq. (9) the forcing condition can be expressed as

$$\tau_H=\rho K_m \frac{C}{\sqrt{2}\delta_i} U_m=\rho u_*^2=\tau_0 \tag{14}$$

Therefore we can express U_m and K_m in the following way:

$$U_m=u_*\sqrt{\frac{\pi}{\sqrt{2}\kappa^2 C}\left[Y_0(C)-\frac{J_0(C)Y_1(C)}{J_1(C)}\right]} \tag{15}$$

$$K_m=\frac{2}{\pi}\frac{U_m\delta_i\kappa^2 J_1(C)}{J_1(C)Y_0(C)-J_0(C)Y_1(C)} \tag{16}$$

References

Arya, S.P., 1999. Air Pollution Meteorology and Dispersion. Oxford University Press.

Abramowitz, M., Stegun, I.A., 1965. Handbook of Mathematical Functions. Dover.

Baranger, P., 1986. Influence des conditions microclimatologiques sur la pollution d'une rue. Ph.D. Thesis, Université de Toulouse.

Berkowicz, R., Hertel, O., Larsen, S.E., Sorensen, M., Nielsen N.N., 1997. Modelling traffic pollution in streets. Technical Report, National Environmental Research Institute.

Berkowicz, R., Hertel, O., Sorensen, N.N. Michelsen, J.A., 1994. Modelling air pollution from traffic in urban areas. In: IMA Conference on Flow and Dispersion Through Groups of Obstacles.

Berkowicz, R., Palmgren, F., Hertel, O., Vignati, E., 1996. Using measurements of air pollution in streets for evaluation of urban airquality—meteorological analysis and model calculations. Science of the Total Environment 189/190, 259–265.

Berkowicz, R., Ketzel, M., Vachon, G., Louka, P., Rosant, J.M., Mesteyer, P.G., Sini, J.F., 2002. Examination of traffic pollution in a street canyon using the Nantes 99 experimental data and comparison with model results. Water, air and Soil pollution 2, 311–324.

Carissimo, B., Dupont, E., Musson-Genon, L., Marchand, O., 1995. Note de principe du code Mercure version 3.1. Technical Report HE-3395007B, EDF-DER.

Garbero, V., Salizzoni, P., Soulhac, L., 2010. Experimental study of pollutant dispersion within a network of streets. Boundary-Layer Meteorology 136, 457–487.

Hargreaves, D.M., Baker, C.J., 1997. Gaussian puff model of an urban street canyon. Journal of Wind Engineering & Industrial Aerodynamics 71, 927–939.

Kumar, P., Fennell, P., Britter, R., 2008. Effect of wind direction and speed on the dispersion of nucleation and accumulation mode particles in an urban street canyon. Science of the Total Environment 402, 82–94.

Launder, B.E., 1978. Heat and Mass transport. In: Bradshaw, P. (Ed.), Topics in Applied Physics 12—Turbulence. Springer, Berlin.

Martin, D., Price, C.S., White, I.R., Nickless, G., Petterson, K.F., Britter, R.E., Robins, A.G., Belcher, S.E., Barlow, J.F., Neophytou, M., Arnold, S.J., Tomlin, A.S., Smalley, R.J., Tate, J.E., Shallcross, D.E., 2009. Urban tracer dispersion experiments during the second DAPPLE field campaign in London 2004. Atmospheric Environment 44, 3043–3052.

Milliez, M., Carissimo, B., 2007. Numerical simulations of pollutant dispersion in an idealized urban area, for different meteorological conditions. Boundary-Layer Meteorology 122, 321–342.

Pavageau, M., Schatzmann, M., 1999. Wind tunnel measurements of concentration fluctuations in an urban streetcanyon. Atmospheric Environment 33 (24–25), 3961–3971.

Salizzoni, P., 2006. Mass and momentum transfer in urban boundary layer. PhD Thesis, Politecnico di Torino - Ecole Centrale de Lyon.

Salizzoni, P., Soulhac, L., Mejean, P., 2009. Street canyon ventilation and atmospheric turbulence. Atmospheric Environment 43, 5056–5067.

Soulhac, L., 2000. Modélisation de la dispersion atmosphérique à l'intérieur de la canopéeurbaine. Ph.D. Thesis, Ecole Centrale de Lyon.

Soulhac, L., Garbero, V., Salizzoni, P., Mejean, P., Perkins, R., 2009. Flow and dispersion in street intersections. Atmospheric Environment 43, 2981–2996.

Soulhac, L., Perkins, R.J., Salizzoni, P., 2008. Flow in a street canyon for any external wind direction. Boundary-Layer Meteorology 126, 365–388.

Tomlin, A.S., Smalley, R.J., Tate, J.E., Barlow, J.F., Belcher, S.E., Arnold, S.J., dobre, A., Robins, A., 2009. A field study of factors influencing the concentrations of traffic-induced pollutant in the vicinity of a complex urban junction. Atmospheric Environment 43, 5027–5037.

Vardoulakis, S., Fisher, B., Pericleous, K., Gonzales-Flesca, N., 2003. Modelling air quality in street canyons: a review. Atmospheric Environment 37, 155–182.